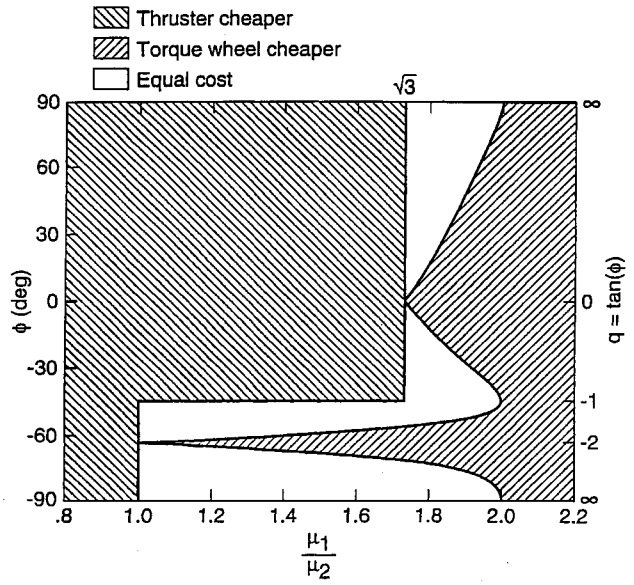

Fig. 1 Optimal control of a rigid body.

Conclusions

It has been shown that for a rigid body with dissimilar actuators that mixed control strategies are nonoptimal. From there it was determined which control is optimal for any given cost weighting and maneuver. This was verified by direct evaluation of the cost of each control. Finally, the optimal control choices for a variety of maneuver/cost weighting pairs were presented. In particular, it was shown when the nondimensional ratio of costs was either more than 2 or less than 1 that the lower weighted control was cheaper regardless of the maneuver. Otherwise, the optimal control choice depended on the maneuver.

References

[1]Bryson, A. E., and Ho, Y., *Applied Optimal Control*, Hemisphere, Washington, DC, 1975, p. 1.

[2]Redmond, J., and Silverberg, L., "Fuel Consumption in Optimal Control," *Journal of Guidance, Control, and Dynamics*, Vol. 15, No. 2, 1992, pp. 424–430.

[3]Silverberg, L., and Redmond, J., "Fuel Optimal Propulsive Reboost of Flexible Spacecraft," *Journal of Guidance, Control, and Dynamics*, Vol. 16, No. 2, 1993, pp. 424–430.

[4]Neustadt, L. W., "Minimum Effort Control Systems," *SIAM Journal of Control*, Vol. 1, No. 1, 1962, pp. 16–31.

Line-of-Sight Guidance for Descent to a Minor Solar System Body

Colin R. McInnes* and Gianmarco Radice†
University of Glasgow,
Glasgow G12 8QQ, Scotland, United Kingdom

Introduction

A PRELIMINARY analysis of line-of-sight guidance for soft landing a payload on a minor solar system body is presented. A simple kinematic model is developed that is used to assess the lander requirements in terms of thrust induced acceleration, thrust vector pointing, and total maneuver Δv. Issues relating to sensor requirements and onboard implementation are also briefly discussed.

Various schemes have been investigated for soft landing payloads on the surface of small asteroids and comets.[1–3] Given the extremely low gravitational acceleration of such bodies, methods have been proposed that are quite different to conventional gravity turn guidance[4] used for powered descent to lunar or planetary surfaces. Surface beacons, descent synchronous with the body rotation, and tethering the vehicle to the asteroid or cometary surface have all been considered.[2,3]

In this Note a scheme is outlined whereby the lander is guided to the desired landing location along a line of sight to the landing location from an orbiter. The orbiter is assumed to have high-resolution imaging capability that may be used to track a desired landing location previously surveyed by the orbiter. The orbiter observes both the lander and the landing location and guides the lander onto the line of sight. A prescribed velocity profile along the line of sight is defined to ensure soft landing. By utilizing available sensors on the orbiter the method allows, in principle, precision soft landing of payloads without the need for complex sensors on the lander. The method may also be used for targeting surface penetrators on hyperbolic fly pasts.

System Kinematics

An orbiter S orbits a small asteroid of radius R at some fixed altitude h above the equator, as shown in Fig. 1. The asteroid is assumed to be spherical and to have a uniform spin rate Ω. After rising above the local horizon of the landing location L, a line of sight is established to an equatorial landing location and the lander P detached from the orbiter. The position vectors of the landing location $\boldsymbol{R}$ and orbiter $\boldsymbol{r}$ may be written in terms of unit vectors $\boldsymbol{i}$ and $\boldsymbol{j}$ as

$$\boldsymbol{R} = R\cos\lambda\boldsymbol{i} + R\sin\lambda\boldsymbol{j} \tag{1a}$$

$$\boldsymbol{r} = (R+h)\cos(\omega t + \theta_0)\boldsymbol{i} + (R+h)\sin(\omega t + \theta_0)\boldsymbol{j} \tag{1b}$$

where the angular velocity of the orbiter relative to the spinning asteroid surface is given by

$$\omega = \sqrt{\frac{GM}{(R+h)^3}} - \Omega, \qquad \omega > 0 \tag{2}$$

and GM is the product of the gravitational constant and the asteroid mass. The line-of-sight vector $\boldsymbol{s}$ from the landing location to the orbiter is then given by

$$\boldsymbol{s} = [(R+h)\cos(\omega t + \theta_0) - R\cos\lambda]\boldsymbol{i} + [(R+h)\sin(\omega t + \theta_0) - R\sin\lambda]\boldsymbol{j} \tag{3}$$

where θ_0 defines the initial orbiter location.

To calculate the required lander acceleration, the line-of-sight angle ϕ must now be obtained. This angle can be obtained from

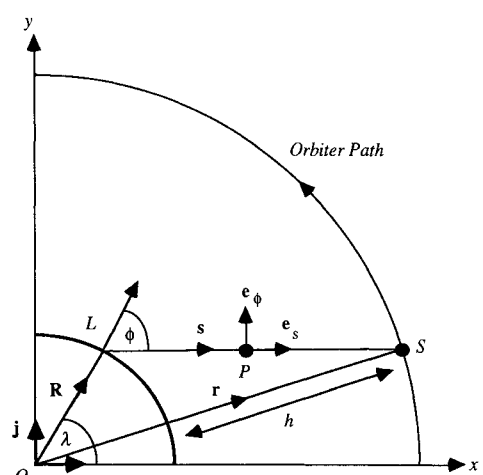

Fig. 1 Schematic geometry of line-of-sight descent.

Received July 12, 1995; revision received Nov. 8, 1995; accepted for publication Nov. 10, 1995.

*Lecturer, Department of Aerospace Engineering.

†Research Assistant, Department of Aerospace Engineering; on leave of absence from Politecnico di Milano, Milan, Italy.

the scalar product of the landing location position vector $\boldsymbol{R}$ and line-of-sight vector $\boldsymbol{s}$ as

$$\cos\phi = \boldsymbol{s}\cdot\boldsymbol{R}/|\boldsymbol{s}||\boldsymbol{R}| \tag{4}$$

Substituting for the appropriate vectors, the line-of-sight angle is

$$\cos\phi = \frac{(R+h)\cos[(\omega t+\theta_0)-\lambda]-R}{\sqrt{(R+h)^2+R^2-2R(R+h)\cos[(\omega t+\theta_0)-\lambda]}} \tag{5}$$

This function may be differentiated to obtain the angular rate and acceleration of the line of sight as the orbiter rises above the horizon and passes over the landing location.

Now that the lander has been constrained to the line of sight, the motion of the lander along the line of sight can be considered. To ensure a soft landing, a prescribed slant-range profile $s(t)$ will be used that satisfies the boundary conditions of the problem. Given that there are four boundary conditions, a cubic function will be used, viz.,

$$s(t) = s_0 + s_1 t + s_2 t^2 + s_3 t^3 \tag{6}$$

If the descent time is defined to be τ, then the following conditions are required:

$$s(0) = s_0 \tag{7a}$$

$$\dot{s}(0) = \dot{s}_0 \tag{7b}$$

$$s(\tau) = 0 \tag{7c}$$

$$\dot{s}(\tau) = 0 \tag{7d}$$

where s_0 is the initial line-of-sight distance and $\dot{s}_0$ is the initial velocity component of the orbiter/lander combination along the line of sight at the initiation of the descent. The coefficients of the cubic function can now be obtained using Eqs. (7). It is found that the slant-range profile is of the form

$$s(t) = s_0 + \dot{s}_0 t + (3s_0 + 2\dot{s}_0\tau)(t/\tau)^2 + (2s_0 + \dot{s}_0\tau)(t/\tau)^3 \tag{8}$$

Again, this function may be differentiated to obtain the prescribed lander velocity and acceleration components along the line of sight from separation to soft landing.

Required Lander Acceleration

Using the preceding analysis the requirements on the lander may be obtained by explicitly calculating the thrust induced acceleration to follow the prescribed descent profile along the line of sight. The lander acceleration can be obtained by resolving in components along the line-of-sight and transverse directions. Therefore, using the unit vectors attached to the lander, as shown in Fig. 1, the thrust induced acceleration components may be conveniently written as

$$a_s = \ddot{s} - s\dot{\phi}^2 + \boldsymbol{g}\cdot\boldsymbol{e}_s \tag{9a}$$

$$a_\phi = s\ddot{\phi} + 2\dot{s}\dot{\phi} + \boldsymbol{g}\cdot\boldsymbol{e}_\phi \tag{9b}$$

where $\boldsymbol{g}$ is the local gravitational acceleration. The required derivative terms can now be obtained from Eqs. (5) and (8) so that the line-of-sight and lateral acceleration components can be calculated.

A typical line-of-sight descent is illustrated in Fig. 2, where the lander and orbiter are shown midway through the descent. The orbiter is parked on a 10-km circular orbit above a 25-km asteroid. The asteroid is taken to have a density of 1 g cm^{-3} and a spin period of 10 h. The descent begins when the orbiter rises above the local horizon of the landing location. The lander then follows the line-of-sight landing 89.4 min after separation. The total Δv for the maneuver is 35.6 ms^{-1} with a maximum required acceleration of 0.012 ms^{-2} just prior to landing. It is found that the thrust vector initially gives a small acceleration component down the line of sight to set the lander moving relative to the orbiter. For most of the descent, however, the thrust vector is directed along the line of sight to the orbiter to brake continuously and keep the lander on the line of sight. Alternatively,

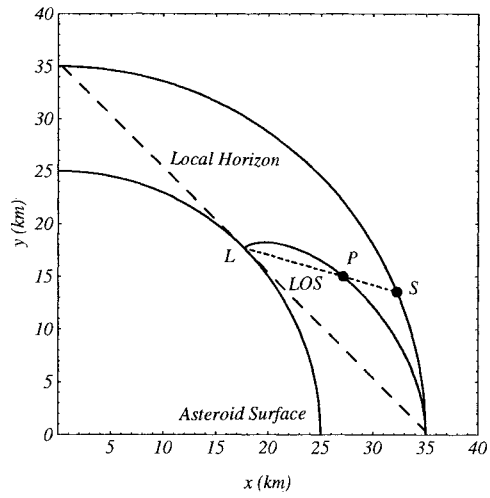

Fig. 2 Lander descent path.

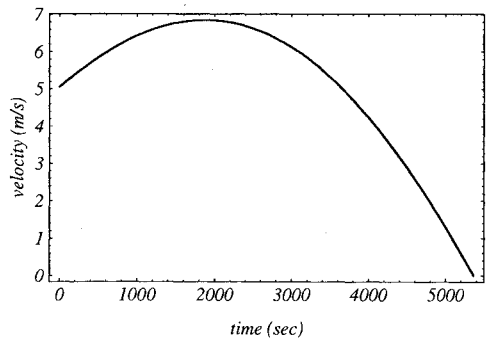

Fig. 3 Surface relative velocity profile.

the lander attitude may be fixed along the line of sight with body fixed thrusters providing radial and lateral accelerations independently. Lastly, the surface relative velocity profile is shown in Fig. 3 where it can be seen that the lander velocity increases slightly during the initial part of the descent. This is because of the descent path being constrained to the line of sight.

Onboard Implementation

It has been assumed that the orbiter possesses a high-resolution imaging system with a scanning platform as part of its science payload, in addition to the lander. Therefore, one of the main elements of the science payload may also be used for descent guidance purposes. This would require onboard software to continuously identify the landing location from camera images. For a typical wide-angle camera[1] with a footprint of 48 μrad and field of view of 2.8×2.8 deg, objects as small as 1.2 m may, in principle, be resolved at the initiation of the descent already discussed. Prior to landing, when the orbiter is directly over the landing location the resolution increases to 0.5 m, in principle, allowing precision guidance to the desired landing location.

For the orbiter to track the lander, a strobe or other visual beacon would be required on the lander to allow resolution of the lander against the asteroid surface. The off-beam distance detected by the orbiter would then be used to generate lateral acceleration commands to be downlinked to the lander. Such schemes are well understood for line-of-sight guided weapon systems.

Although a prescribed slant-range profile has been used in the analysis for convenience, it is, in principle, possible to use a prescribed slant-range rate profile as a function of slant range as measured by the lander. This would then allow a fully closed-loop system with line-of-sight guidance commands being downlinked from the orbiter and slant-range rate being measured and controlled by the lander.

Conclusions

The method outlined in this Note appears to provide scope for precision landing of payloads on minor solar system bodies using

an orbiter as a reference to generate a line of sight to the landing location. By utilizing already existing visual sensors on the orbiter, the lander can be equipped with relatively simple radar sensors for slant range and slant range-rate measurements. Lastly, although the method has been considered for soft landing of payloads, it may, in principle, be used for accurate targeting of impacting penetrators during hyperbolic fly pasts.

References

[1]Noton, M., "Orbit Strategies and Navigation near a Comet," *ESA Journal*, Vol. 16, 1992, pp. 349–362.

[2]De Lafontaine, J., "Autonomous Spacecraft Navigation and Control for Comet Landing," *Journal of Guidance, Control, and Dynamics*, Vol. 15, No. 3, 1992, pp. 567–576.

[3]Champetier, C., Regnier, P., Serrano, J. B., and de Lafontaine, J., "Evaluation of Autonomous GNC Strategies for the Rosetta Interplanetary Mission," *Proceedings of the IFAC Automatic Control in Aerospace Conference*, Pergamon, London, 1992, pp. 339–353.

[4]McInnes, C. R., "Non-linear Transformation Methods for Gravity Turn Descent," Dept. of Aerospace Engineering, Rept. 9506, Univ. of Glasgow, Scotland, UK, Jan. 1995.

New Numerical Method Improving the Integration of Time in KS Regularization

J. M. Ferrándiz*
Universidad de Alicante, E-3080 Alicante, Spain
and
J. Vigo-Aguiar†
Universidad de Salamanca, E-37008 Salamanca, Spain

I. Introduction

THE change of the independent variable $dt = c_\alpha r^\alpha d\tau$ has often been used in modern celestial mechanics (e.g., Ref. 1). Constants α and c_α are usually given values so that τ becomes an anomaly: eccentric, true, or intermediate[2] for $\alpha = 1, 2$, or $\frac{3}{2}$, respectively. The original Sundman[3] choice $\alpha = 1$ later was successfully used, together with KS transformation, in obtaining harmonic oscillator equations for the two-body problem, as described in Stiefel and Scheifele.[4]

The use of such transformations for the numerical propagation of satellite orbits introduces a new source of error arising from the inaccuracy in the time computation. It may become too relevant when precise ephemerides are required and override the benefits of the regularization. Therefore, additional techniques are necessary to improve the numerical integration of the physical time.

Among these techniques, the integration of a time element (i.e., a constant or linear function of the independent variable), instead of time, may produce an increase in accuracy by a factor reaching the order of the dominant perturbation J_2, at most. If the eccentric anomaly is taken as an independent variable, an alternative procedure comes from replacing the equation for t' by a new equation for $t''' + t'$ since that expression is constant in the unperturbed case[5] and, therefore, varies slowly. Moreover, the use of a multistep code for third-order equations provides an extra factor h^2 in the truncation error, h being the stepsize.

It is also known that the numerical integration of the KS coordinates, as well as the time, can be improved using special codes such as the Bettis[6] code, which allow the exact integration (i.e., without truncation error) of oscillations in one or several frequencies.

In this Note we introduce a special algorithm for third-order equations in the form $t''' + w^2 t' = f$ that generalizes the Bettis method and that is capable of exactly integrating the unperturbed problem. In this way, the ideas of the last two approaches are brought together. This new algorithm is based on the authors' previous results[7,8] for the adaptation of unspecified multistep codes that ensure the essential properties of the method, in particular order, convergence and expression of the local truncation error. The computational cost is the same as that of any classical multistep code of constant step; the only difference appears in the computation of coefficients, at the beginning of the integration.

In Sec. III, we present experiments relative to numerical propagation of satellite orbits for the J_2 problem. The results of the proposed approach are compared with those corresponding to other known KS systems, including elements and time element. Significant gains in accuracy in determining the physical time are obtained, especially in the case of highly eccentric orbits.

II. Description of the Numerical Integrator

Recently the authors introduced a general procedure for the construction of multistep codes that integrate initial value problems (IVPs) whose differential equation is given in the form $L(y) = f(x, y)$, where $L(y)$ is a linear differential operator with constant coefficients. The codes are capable of integrating the homogeneous part ($f = 0$) exactly to within machine roundoff error. A complete study of these algorithms exceeds the limits of a Note and can be found in Refs. 7 and 8.

When the procedure is applied to an IVP of the form

$$t''' + \omega^2 t' = f \qquad t(0) = t_0, \quad t'(0) = t_0', \quad t''(0) = t_0'' \tag{1}$$

a new method is obtained with the expression

$$y_p - a y_{p-1} + a y_{p-2} - y_{p-3} = h^3 \sum_{j=0}^{k} \beta_j \nabla^j f_{p-i} \qquad a = 1 + 2\cos\omega h \tag{2}$$

where ω is the constant frequency of the fundamental oscillations and h the (constant) stepsize. The β_j coefficients correspond to the Taylor expansion of the functions

$$G_i = \frac{1 - a(1-\xi) + a(1-\xi)^2 - (1-\xi)^3}{(1 - i\xi)[\log(1-\xi)^3 + h^2 \log(1-\xi)]} \tag{3}$$

with $i = 1$ for the explicit (predictor) algorithm and $i = 0$ for the implicit (corrector) case. Their value depends on ωh, but the computational cost of the methods is the same as any standard multistep code, because the coefficients β_j have only been computed once.

Following Ref. 8, the properties of the method can be established in the following theorem.

Theorem: Method (2) is convergent with local truncation error

$$\mathcal{L}_A(t, h)(x) = h^{k+4} C_{k+1}\{(D^{k+4} + D^{k+2})t(x)\} + \mathcal{O}(h^{k+5}) \tag{4}$$

where C_{k+1} is the error constant and D the derivation operator. Then the method integrates any function that is a linear combination of the following set:

$$\sin\omega x, \quad \cos\omega x, \quad 1, \quad x, \ldots, x^k \tag{5}$$

without local truncation error.

III. Integration of the Main Problem of Satellite in KS Variables

In this section we present the results of the integration of the main satellite problem in KS variables (see Ref. 4), computing the

Received July 20, 1995; revision received Dec. 15, 1995; accepted for publication Dec. 18, 1995.

*Professor, Department of Applied Mathematics, P.O. Box 99.
†Associate Professor, Department of Pure and Applied Mathematics.